Capacitively Tuned Electrical Coupling for Reconfigurable Coaxial Cavity Bandstop Filters

Akash Anand and Xiaoguang Liu
Department of Electrical and Computer Engineering, University of California Davis, USA
akaanand@ucdavis.edu and lxgliu@ucdavis.edu

***Abstract*—A coaxial-cavity two-pole bandstop filter with continuously tunable center frequency and bandwidth is presented. The center frequency is tuned by capacitively loading the coaxial cavity with surface mount varactors. The bandwidth is reconfigured by controlling the energy coupled into the resonator by another surface mount varactor. Measured results show good agreement with simulation. The filter tunes from 0.77 GHz to 1.5 GHz. The 3-dB bandwidth tuning range is approximately 20 MHz to 85 MHz in the lower frequency range and approximately 50 MHz to 300 MHz in the upper frequency range. As an example, a frequency range of 0.77–1.25 GHz with constant bandwidth of 83 MHz is demonstrated with stopband attenuation of at least 18 dB. At larger 3-dB bandwidths, stopband attenuation up to 70 dB is measured.**

***Index Terms*—combline filter, evanescent-mode filter, tunable filters, bandstop filter, waveguide filters**

I. Introduction

As the frequency spectrum gets more crowded with the growing number of transmitters, chances of harmful interference are becoming ever greater. These interferes may desensitize or raise the noise figure of receiving systems. One possible solution is to use bandstop filters to reject interfering signals. Moreover, the frequency and the bandwidth of the interferes may vary dynamically over time. In such environments, a fully-reconfigurable bandstop filter (BSF) becomes essential where both center frequency and bandwidth may be tunable. Reconfigurable BSFs can also be used to reject unwanted harmonics or unwanted signals generated by non-linear devices, such as harmonics in power amplifiers [1].

Recently, fully-reconfigurable BSFs have been investigated in the form of planar microstrip filters [2]–[4]. These planar filters tune both the center frequency and bandwidth using surface mount solid state diodes. To get better attenuation level, 3-D cavities with higher unloaded quality factor are preferable. Typically, apertures are created in 3-D resonant cavities to couple the signal energy into the resonators to give a bandstop response, such as in [5], [6]. In [5], only the center frequency is tunable. In [6], the bandwidth is tuned by pole allocation at the expense of reduced rejection level: increasing the bandwidth decreases the stopband rejection level.

The energy coupled into the resonators needs to be tunable to realize reconfigurable bandstop filters. But it is difficult to electrically tune the coupling in these 3-D bandstop resonators because inductive coupling (apertures openings) into the cavities is fixed, and electrical coupling is typically not convenient to implement since the resonators and input/output feeds are on two different substrates [5], [6]. For this reason,

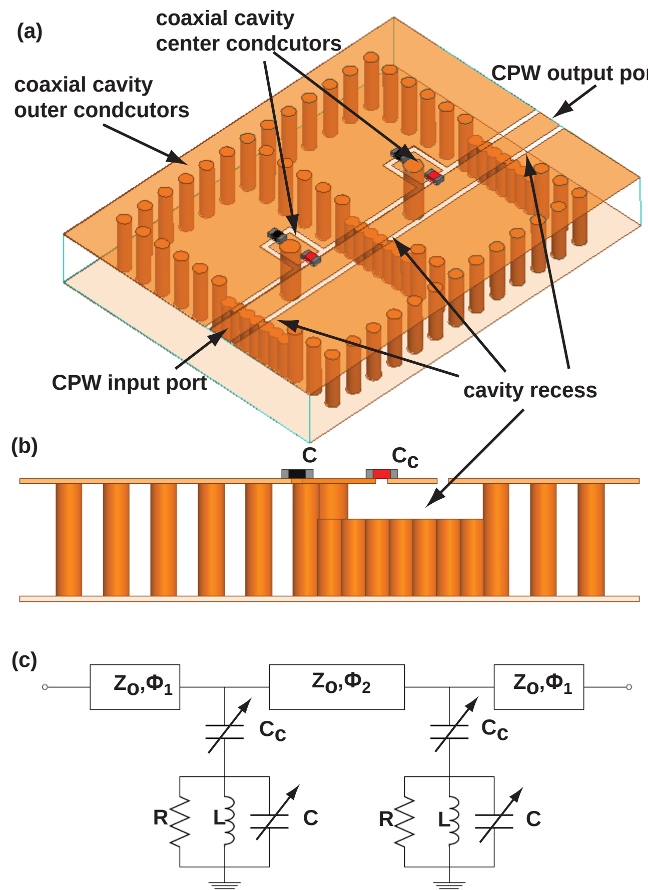

Fig. 1. (a) Top view and (b) side view of proposed two-pole bandstop filter. (c) Lump-distributed model for bandstop filter.

very little work has been done to develop fully-reconfigurable bandstop filters with cavity resonators. In this work however, the input/output feed lines are integrated together with the coaxial cavities in one substrate to implement tunable capacitive coupling. Figure. 1(a) shows the proposed structure where the input signal passes through a coplanar waveguide (CPW) to the output at all frequencies, except at the resonance where the signal is capacitively coupled into the resonators, creating a notch response.

II. Design

A. Bandstop Resonator

The proposed substrate-integrated coaxial-cavity resonators are based on the design presented in [7]–[9]. Metallic vias

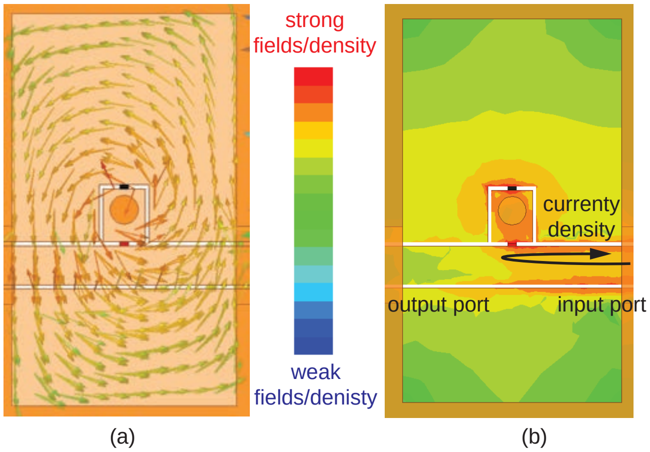

Fig. 2. HFSS simulation of a single bandstop resonator at resonant frequency. Results show the (a) magnetic fields excited in the substrate and (b) the current density flows from the input port into the resonator.

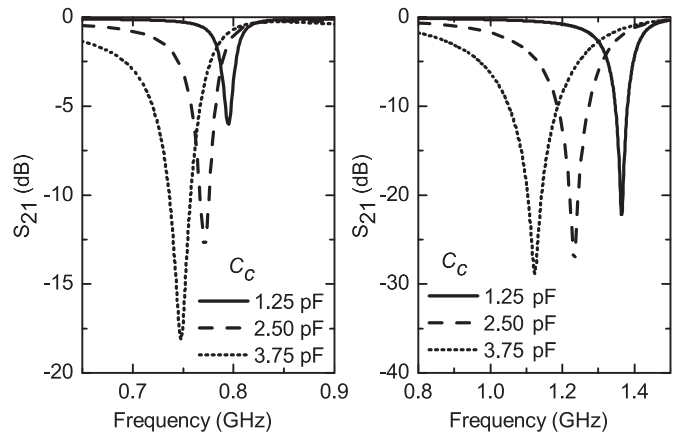

Fig. 3. Simulation from HFSS shows tunable bandwidth at the (a) lower tunable frequency and at the (b) higher tunable frequency.

created in the substrate forms the rectangular cavity's outer conductor and the inner conductor (center post) in Fig. 1(a). The center post shorts the bottom and the top of the cavity while a square ring gap on the surface isolates the center post from the rest of the cavity's top. Similar to the work in [8], surface mount varactors (C) load the coaxial resonators and tune the center frequency. A CPW transmission line integrated on the cavity's top surface is used as the input and output ports. At resonance, the energy is capacitively coupled into the resonators through another surface mount varactor (C_c). Fig. 1(b) shows the side view of the bandstop filter, where the recess in the cavity's wall prevents the CPW transmission line from shorting.

Fig. 2 shows a one-pole bandstop filter (or a bandstop resonator). For simplicity, a rectangular wall is used instead of metallic vias to form the cavity's outer conductor. This structure is simulated in a full-wave electromagnetic simulator (Ansys HFSS) at the cavity's resonant frequency. As expected for coaxial resonators, Fig. 2(a) shows the magnetic field in the substrate circles around the center post: fields are strongest closest to the post and weaker closer to the outer conductor wall. Fig. 2(b) shows the current density on the top surface of the cavity. It is evident from Fig. 2(b) that at the resonance, energy is excited into the cavity from the CPW's input port and is coupled into the resonator through C_c. Current density flowing into the output port is much weaker.

Fig. 3 shows the simulated s-parameters for the bandstop resonator in Fig. 2 with $C = 2.5$ pF and $C = 10$ pF and $C_c = 1.25$ pF, 2.50 pF and 3.75 pF. When $C = 10$ pF, the resonant frequency is around 0.77 GHz and increases to around 1.3 GHz when $C = 2.5$ pF. As C_c increases, more energy is coupled into the resonators, and thus bandwidth increases as C_c increases. Table I summaries the resonant frequencies at various C and C_c values. Note that the resonant frequency also depends slightly on C_c. The resonator dimensions are given in section III.

TABLE I
RESONANT FREQUENCY OF SIMULATED RESONATOR IN GHz

	$C = 2.5$ pF	$C = 5.0$ pF	$C = 7.5$ pF	$C = 10.0$ pF
$C_c = 1.25$	1.34	1.06	0.90	0.79
$C_c = 2.50$	1.23	1.00	0.86	0.77
$C_c = 3.75$	1.12	0.95	0.83	0.75

B. *Two-pole Bandstop Filter*

The proposed two-pole bandstop filter design is shown in Fig. 1(a) and the lump element model for the filter is shown in Fig. 1(c). The impedance of the CPW line is $Z_o = 50\Omega$. Ideally, for bandstop filters, the two resonators should be separated by a quarter-wave length transmission line ($\phi_2 = 90\,°$), which serves as an inverter [5]. Results from [5] show that rejection level degrades as ϕ_2 deviates from $90\,°$. But, simulation also shows that the upper passband degrades as ϕ_2 increases. Thus there is a compromise between better stopband rejection or better upper passband: $\phi_2 = 90\,°$ results in optimal stopband rejection while smaller ϕ_2 results in higher upper passband. The frequency response for the two-pole bandstop filter is presented in section III.

III. EXPERIMENTAL VALIDATION

Fig. 4(a) and (b) show the fabricated two-pole bandstop filter with and without the surface mount diodes. A 6.35-mm thick Rogers TMM3 substrate is used to fabricated the filter. The dimensions of the resonator is given in the figure. The center post and the outer vias have a diameter of about 1 mm and are copper plated. Compared to Fig. 1(a), two square ring gaps ($3 \times 3\,\text{mm}^2$ and $4 \times 5\,\text{mm}^2$) are created on the top surface in order to isolate dc bias points for the diodes. Eight Skyworks SMV1405 diodes are mounted on each square ring gap for C and two SMV1405 diodes are mounted on each gap for C_c. Ignoring parasitics, C has a range of $\approx$ 2.5–10.6 pF and C_c has a range of $\approx$ 1.25–5.3 pF.

Fig. 5 shows measured results for the fabricated two-pole bandstop filter. In Fig. 5(a), the bias voltage for C is held

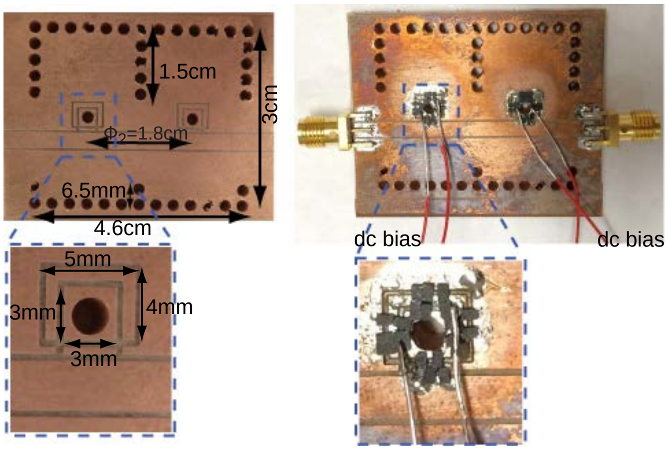

Fig. 4. Fabricated two-pole band stop filter (a) without the surface mount diodes and (b) with the surface mount diodes.

constant while C_c is tuned from 0 V to 10 V. C_c increases as the bias decreases and more energy is coupled into the resonators. Thus bandwidth increases as C_c bias decreases. The stopband attenuation level varies from 34 dB to 70 dB. Note that there is a shift in center frequency as C_c changes. However, since the center frequency is also tunable, this shift can be compensated by tuning C.

Fig. 5(b) and (c) show that a constant center frequency is maintained while the bandwidth is tuned in the frequency range of 0.77–1.25 GHz. The 3-dB bandwidth tuning range is approximately 20–85 MHz in the lower frequency range and approximately 50 MHz to 300 MHz in the higher frequency range. Fig. 5(d) demonstrates a continuously tunable filter from 0.77 GHz to 1.25 GHz with a constant 3-dB bandwidth of 83 MHz.

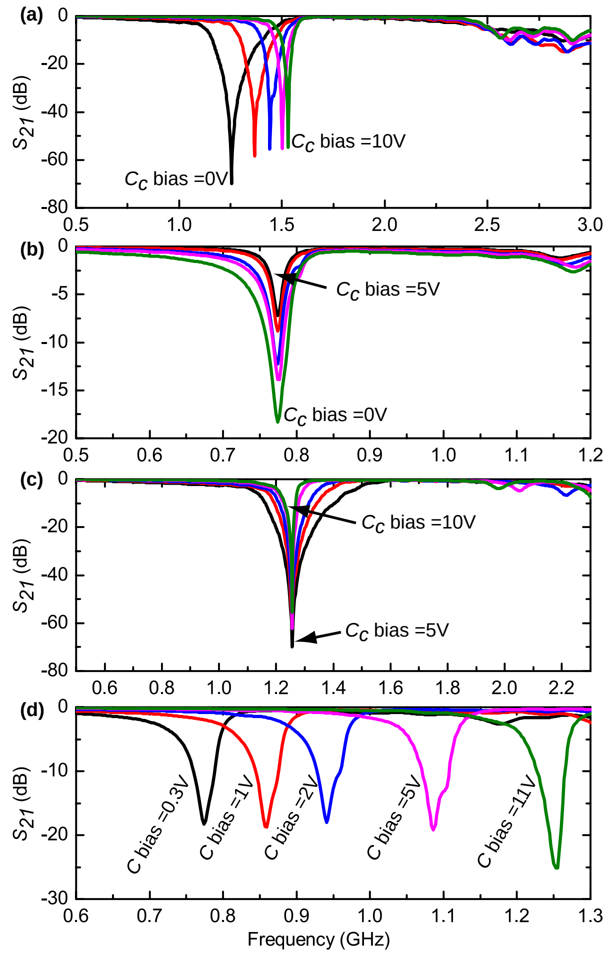

Fig. 5. Measured s-parameters of fabricated filter where (a) shows tunable bandwidth, (b) and (c) show tunable bandwidth at a fixed frequency and (d) shows a constant 83 MHz bandwidth across the tuning range.

IV. Conclusion

This paper presents a coaxial-cavity two-pole bandstop filter with continuously tunable center frequency and bandwidth. The center frequency is tuned by capacitively loading the coaxial cavities with surface mount diodes. The bandwidth is reconfigured by controlling the energy coupled into the resonator by another surface mount diode. Measured results show good agreement with simulation. The filter tunes from 0.77 GHz to 1.5 GHz. The 3-dB bandwidth tuning range is approximately 20 MHz to 85 MHz in the lower frequency range and approximately 50 MHz to 300 MHz in the higher frequency range. As an example, a frequency range of 0.77–1.25 GHz with constant bandwidth of 83 MHz is demonstrated with stopband attenuation of at least 18 dB. At larger 3-dB bandwidths, stopband attenuation up to 70 dB is measured.

References

[1] H.-W. Liu, F. Tong, and X.-H. Li, "Asymmetrical spurline resonator design and its application to power amplifiers," in *IEEE MTT-S International Microwave Workshop Series on Art of Miniaturizing RF and Microwave Passive Components*, Dec 2008, pp. 149–152.

[2] Y.-C. Ou and G. Rebeiz, "Lumped-element fully tunable bandstop filters for cognitive radio applications," *IEEE Transactions on Microwave Theory and Techniques*, vol. 59, no. 10, pp. 2461–2468, Oct 2011.

[3] Y.-H. Cho and G. Rebeiz, "Two- and four-pole tunable 0.7-1.1-ghz bandpass-to-bandstop filters with bandwidth control," *IEEE Transactions on Microwave Theory and Techniques*, vol. 62, no. 3, pp. 457–463, March 2014.

[4] A. Guyette, "Varactor-tuned bandstop filters with tunable center frequency and bandwidth," in *Wireless Information Technology and Systems (ICWITS), 2010 IEEE International Conference on*, Aug 2010, pp. 1–4.

[5] A. Anand, Y. Liu, and X. Liu, "Substrate-integrated octave-tunable combline bandstop filter with surface mount varactors," in *Wireless Symposium (IWS), 2014 IEEE International*, March 2014, pp. 1–4.

[6] E. Naglich, J. Lee, D. Peroulis, and W. Chappell, "High-q tunable bandstop filters with adaptable bandwidth and pole allocation," in *Microwave Symposium Digest (MTT), 2011 IEEE MTT-S International*, June 2011, pp. 1–1.

[7] A. Anand, J. Small, M. S. Arif, M. Sinani, D. Peroulis, and X. Liu, "A novel high-qu octave-tunable resonator with lumped tuning elements," in *IEEE MTT-S International Microwave Symposium Digest*, June 2013, pp. 1–3.

[8] A. Anand, J. Small, D. Peroulis, and X. Liu, "Theory and design of octave tunable filters with lumped tuning elements," *IEEE Transactions on Microwave Theory and Techniques*, vol. 61, no. 12, pp. 4353–4364, Dec 2013.

[9] A. Anand and X. Liu, "Substrate-integrated coaxial-cavity filter with tunable center frequency and reconfigurable bandwidth," in *Wireless and Microwave Technology Conference (WAMICON), 2014 IEEE 15th Annual*, June 2014, pp. 1–4.

978-1-4799-8275-2/15/$31.00 ©2015 IEEE